

## The interactions between tetrapyrrolyl porphyrin and viologen units covalently linked to polymers

A. Bartczak<sup>a</sup>, Y. Namiki<sup>b</sup>, D.-J. Qian<sup>b</sup>, J. Miyake<sup>b</sup>,  
A. Boguta<sup>a</sup>, J. Goc<sup>a</sup>, J. Łukasiewicz<sup>a</sup>, D. Frąckowiak<sup>a,\*</sup>

<sup>a</sup> Faculty of Technical Physics, Poznań University of Technology, Nieszawska 13A, 60-965 Poznań, Poland

<sup>b</sup> Tissue Engineering Research Center, National Institute of Advanced Science and Technology, 3-11-46 Nakoji, Amagasaki, Hyogo 661-0974, Japan

Received 1 January 2003; received in revised form 6 March 2003; accepted 2 April 2003

### Abstract

The spectral properties of tetrapyrrolyl porphyrin covalently linked to polymer and copolymer of porphyrin–viologen in dimethylformamide solutions were compared. Many more viologen groups than tetrapyrrolyl chromophores were linked to polymer.

The viologen is an electron acceptor. The processes of deactivation of the excitation energy with and without addition of electron donors (ethylenediaminetetraacetic acid or triethanolamine) to the solution were investigated. In order to establish the fate of the absorbed energy the absorption, fluorescence, fluorescence excitation, as well as steady state and time-resolved photothermal spectra were measured. The yield of porphyrin triplet state generation was established. The excitation of reduced monomer of viologen (at 390 nm) was followed by 530 nm fluorescence due to some form of viologen. It is not excluded that this emission could be due to excimeric form of viologen. From absorption spectra of irradiated samples with the addition of electron donors it was shown that the electron transfer between porphyrin and methyl viologen units linked to polymer is not efficient. This transfer is more efficient between porphyrin and viologen added to solution. This shows that for electron transfer, shorter distance between porphyrin and viologen than that between those attached to polymer groups is necessary.

In samples without viologen the singlet excitation energy can be transferred from the excited state of polymer or from a weakly bound to a more strongly bound porphyrin state which is responsible for fluorescence emission. Fluorescence emission competes with processes of intersystem ( $S_1 \rightarrow T_1$ ) transition and thermal deactivation. The laser induced optoacoustic spectra (LIOAS) were measured at various temperatures in order to establish conditions in which the volume change of the illuminated samples could be neglected and measured signals were caused only by triplet states thermal deactivation. The addition of the electron donor to the solution has an influence on the yield and decay time of the triplet states of porphyrin units attached to polymer. Oxygen changed the decay time of triplet states. The schemes describing the fate of excitation in both types of samples were proposed. The data obtained can be useful in the construction of a system for conversion of light energy into electrical energy, in hydrogen production and the application of dyes in photodynamic therapy. The investigated systems can also be treated as a simplified model of photosynthetic apparatus of organisms.

© 2003 Elsevier Science B.V. All rights reserved.

**Keywords:** Charge transfer; Excitation electron transfer; Fluorescence; Photothermal spectroscopy; Polymer; Porphyrin; Triplet state; Viologen

### 1. Introduction

Porphyrin-based covalently linked ensembles containing an electron donor or acceptor or the systems containing regularly arranged dye molecules can be used as a model of a reaction center or antenna system of photosynthetic organisms [1–4], or as a part of the system working as a converter of light energy into electrical energy [5]. The system which was investigated can also be useful in the establishment of a possible application of porphyrin dyes in the photodynamic diagnosis and photodynamic therapy of cancer [6,7] as well as in the arrangements for hydrogen production [8–11]. It was shown that other porphyrin–viologen systems

**Abbreviations:** BCP, bromocresol purple; DMF, dimethylformamide; EDTA, ethylenediaminetetraacetic acid; ISC, intersystem crossing; LIOAS, laser induced optoacoustic spectroscopy; PAS, photoacoustic spectroscopy; P, polymer; Por, porphyrin group weakly interacting with polymer; PPor, polymer with tetrapyrrolyl porphyrins; PPorV, copolymer with tetrapyrrolyl porphyrins and viologen; PV, viologen attached to polymer; SWR, short wavelength region 200–350 nm; TEA, triethanolamine; TD, thermal deactivation; V, viologen

\* Corresponding author. Tel.: +48-61-665-31-80;

fax: +48-61-665-32-01.

E-mail address: [frackow@phys.put.poznan.pl](mailto:frackow@phys.put.poznan.pl) (D. Frąckowiak).

can produce hydrogen under steady state irradiation [9]. For the ruthenium–bisviologen complexes the efficient photoinduced hydrogen evolution was also observed [10]. Previously [11] photoinduced hydrogen evolution for porphyrin, viologen and EDTA in solution and in Langmuir–Blodgett films was investigated. In the present work the influence of the linking of porphyrin and viologen to the same polymer on their mutual interactions was investigated. Knowledge of the processes of the transfer of singlet excitation energy between the investigated dyes, the triplet states generation by intersystem crossing (ISC) and their decays, as well as the processes of spontaneous and light generated electron transfer play an important role in all these applications. Ethylenediaminetetracetic acid (EDTA) is widely used in the investigations of electron flow in photosynthetic organisms [12,13]. It has been shown that EDTA could have some influence on the properties of proteins and biological membranes [12,13]. It cannot be excluded that EDTA also has some influence on porphyrin–polymer interactions, but predominantly it serves as an efficient electron donor. In order to compare the influence of the type of electron donor on investigated processes a second electron donor triethanolamine (TEA) was also used. The fate of the absorbed energy can be established by the measurement of absorption, fluorescence, fluorescence excitation, as well as steady state and time-resolved photothermal methods [14,15]. The triplet states are formed predominantly by intersystem crossing between the excited singlet state ( $S_1$ ) and the triplet state ( $T_1$ ). The depopulation of the triplet state by delayed fluorescence and phosphorescence is less efficient than thermal deactivation (TD) from  $T_1$  to ground singlet state ( $S_0$ ). Therefore, the measurement of TD from the triplet state enables an evaluation of the efficiency of the generation of these triplet states by ISC from the excited singlet state [16]. The dynamic of the triplet states generated in polymer chains was investigated by flash photolysis and using photoacoustic calorimetry [17]. It was shown that the triplet states can also be photogenerated in some polymers [17]. Illuminated polymer can also be a source of free charge carriers [17,18]. The process of triplet energy transfer (ET) between various chromophores covalently connected by different bridges strongly depends on a bridge electronic structure, and the distance between donor and acceptor as well as on donor–bridge conformation [19]. The measurements for the same samples of steady state photoacoustic spectra (PAS) and time-resolved laser induced optoacoustic spectroscopy (LIOAS) enable us to distinguish the part of absorbed energy exchanged into heat in all slow TD processes, occurring in the sample, from this part of heat which is due to TD of the triplet states.

It is known that dye aggregation changes the penetration of dye through the biological membrane and dye photochemical properties [20]. The covalent attachment of dyes to polymer preserves the aggregation of dye molecules. The macromolecular systems formed out of polymer with covalently linked dyes can be to some extent the model of biological pigment–protein complexes.

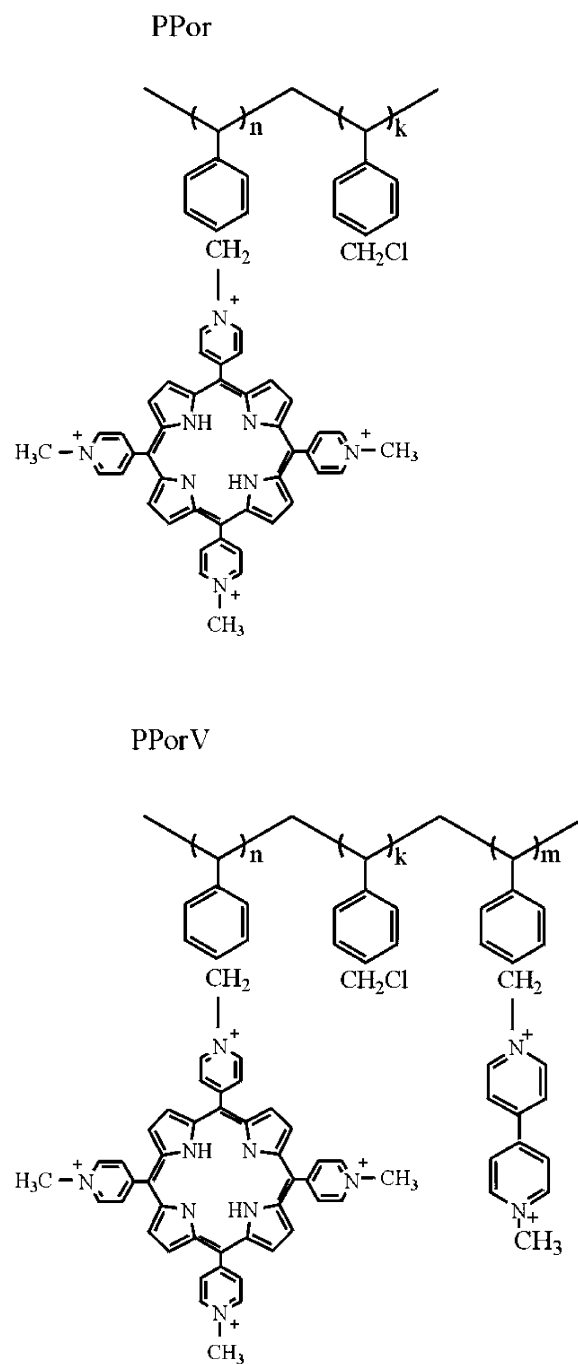


Fig. 1. Structure of investigated samples. PPor-polymer with attached tetrapyrrolic porphyrins, PPorV-copolymer with porphyrin–viologen.

## 2. Materials and methods

The structures of the investigated macromolecules are shown in Fig. 1. The following abbreviations are used: polymer with tetrapyrrolic porphyrins (PPor), copolymer with tetrapyrrolic porphyrins and viologens (PPorV).

The 5,10,15,20-tetra (4-pyridyl)-21H,23H-porphine (TP-P) and poly (vinylbenzyl chloride) (60/40 mixture of three

and four isomers, average  $M_n$  about 55,000, average  $M_w$  about 100,000) were purchased from Aldrich. The 5,10,15-tris methyl (4-pyridyl)-21H,23H-porphine was synthesized by refluxing a TPYP dimethylformamide (DMF) solution for 2 h with a 10-fold excess of methyl iodide as previously [21] described, and obtained by column chromatography (Sephadex LH-20 column, by the elution with water) [22,23]. The polymer PPor (Fig. 1) was synthesized by refluxing DMF solution of poly (vinylbenzyl chloride) and 5,10,15-tris (4-*N*-methylpyridinium)-20-(4-pyridyl)-21H, 23H-porphine for 2 h. After the addition of diethyl ether, the precipitate was collected and washed by a large amount of water to remove unreacted porphyrin.

*N*-Methyl-4,4'-bipyridyl was synthesized according to a method described in literature [24]. Poly (viologen) was obtained by refluxing a methanol/acetonitrile solution of *N*-methyl-4,4'-bipyridyl and poly (vinylbenzyl chloride). The polymer PPorV (Fig. 1) was synthesized by refluxing a DMF solution of poly (viologen) and 5,10,15-tris (4-*N*-methylpyridinium)-20-(4-pyridyl) porphyrin. The product was precipitated by adding diethyl ether and washed by a large amount of water to remove unreacted porphyrin.

According to  $^1\text{H}$  NMR analysis, the ratio of *n:m:k* groups attached to PPorV (Fig. 1) is about 1:30:170. On the basis of UV spectra the ratio of *n:m* groups was estimated to be 1:40, but because of DMF absorption in the short wavelength region, the NMR data appear to be more accurate. The absorption and fluorescence spectra of PPorV suggest that porphyrin units can not be as scarce as indicated in  $^1\text{H}$  NMR. Nevertheless, it is certain that many more viologen than porphyrin groups are attached to PPorV.

The EDTA, TEA and DMF were purchased from POCh., Gliwice (Poland) and used without further purification. The

DMF was used as a solvent. The concentrations of porphyrin units in PPor and PPorV samples were established on the basis of the absorption spectra (Fig. 2). The absorption coefficient at Soret band: for PPor at 428 nm and for PPorV at 454 nm was about  $1.8 \times 10^5 \text{ M}^{-1} \text{ cm}^{-1}$ .

The samples at various times after preparation and samples filtered in order to eliminate long polymer–dyes complexes were also investigated.

The arrangement used for time-resolved photothermal signal measurements was a typical LIOAS apparatus [15,25]. This allow us to distinguish between prompt thermal deactivation effects occurring in a time shorter than the time resolution of the apparatus (in our case about 0.5  $\mu\text{s}$ ), and slow processes which occur in longer times. The samples were illuminated by a sub-nanosecond flash (0.2 ns). The concentrations of the investigated sample and the reference bromocresol purple (BCP) ( $\text{C}_{21}\text{H}_{16}\text{Br}_2\text{O}_5\text{S}$ ) (from RdH Laborchemikalien, Germany) were such that when used for flash wavelength (430 nm), they exhibit the same absorptions. The waveform LIOAS signals for the reference and for the samples were taken. It is known [15] that BCP reference exchanges all absorbed energy into heat in a time shorter than the time resolution of the apparatus. Two methods of signal analysis were used: the first one, proposed by Marti et al. [26], is based on a comparison of the signal maximal amplitude ( $H_{\text{max}}$ ) for the sample and the reference. The second method, elaborated by Rudzki-Small et al. [27] gives values of decay times of TD by the deconvolution of the sample and reference LIOAS signals.

It is known [28] that LIOAS signal consists of two parts: the first one is due to TD of excitation, the second to a change in the volume of macromolecules, occurring as a result of the sample illumination. The second part of the signal

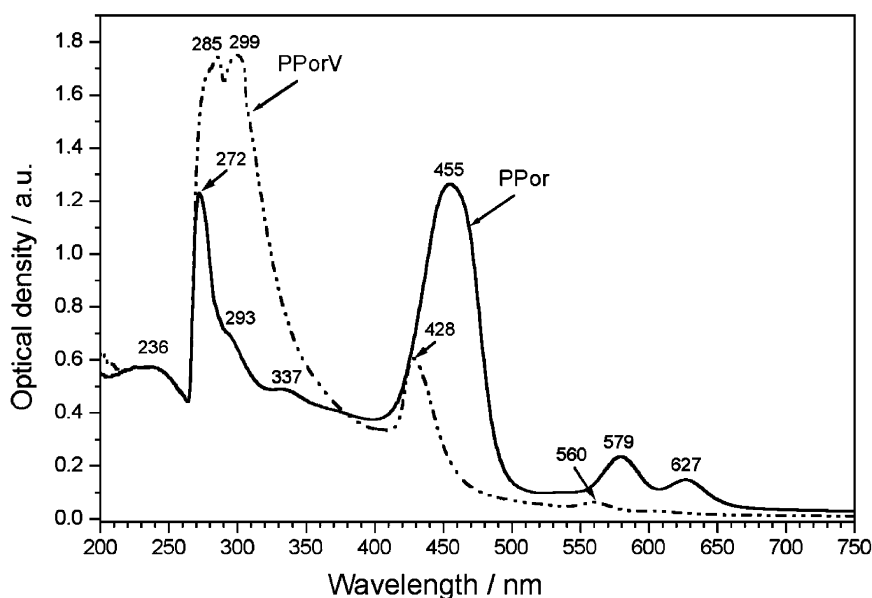


Fig. 2. Absorption spectra of PPor and PPorV just after sample preparation.

depends much more strongly on sample temperature than the first one [28]. Therefore, it is possible to distinguish the contributions from the two effects while measuring LIOAS at various temperatures [28]. A set of such measurements was taken. The influence of oxygen on the triplet states of the samples was established by means of comparison of the signals for the samples bubbled by nitrogen or by oxygen, as well as for the sample being in contact with atmospheric level of oxygen.

The steady state photoacoustic spectra were measured with a single beam photoacoustic spectrometer [29,30]. The comparison of the PAS and LIOAS results supplied information about very slow TD processes, for example, exothermic reactions, occurring in times longer than measured by our LIOAS apparatus (i.e. in times longer than 5  $\mu$ s).

The absorption spectra of the investigated solutions were taken using a Specord M40 spectrometer (Carl Zeiss, Jena, Germany), and fluorescence spectra by means of a Fluorescence Spectrophotometer F4500 (Hitachi, Japan). The absorption of the PPorV samples under Ar atmosphere before and just after 5 min illumination by a 500 W tungsten lamp (without filter, light intensity—1.7 kW/m<sup>2</sup>) was also measured. The same samples with the addition of a small amount of free viologen to the solution, without and with illumination, were also investigated.

### 3. Results

#### 3.1. Absorption spectra

Absorption spectra of PPor and PPorV solutions, just after the preparation of the samples, are shown in Fig. 2. The M band of PPor is located at 272 nm, and a very wide Soret (B) band at 455 nm. In a longer wavelength region, the vibrational bands characteristic for porphyrins are seen. Viologen attachment changes the shape of the spectrum: in the short wavelength region two bands at 285 and 299 nm are located, in a longer wavelength range the band is at 428 nm. During some hours after the sample preparation, the spectra slowly change, reaching the shapes maintained during the time of gathering all spectral results. The Fig. 3A–D shows the absorption of such samples. In PPor spectrum the maximum at 415 nm, characteristics of the dye not attached to polymer, and the maximum at 453 nm, due to porphyrin interacting with polymer, are observed. The vibrational maxima are also slightly changed. The PPorV band exhibits a shoulder at 417 nm, probably due to the dye molecules which interact more weakly with polymer, and the main absorption maximum is at 426 nm.

In order to establish why the spectra presented in Fig. 3 differ from the spectra in Fig. 2, the samples with absorption such as in Fig. 3 were filtered through filter paper. As a result

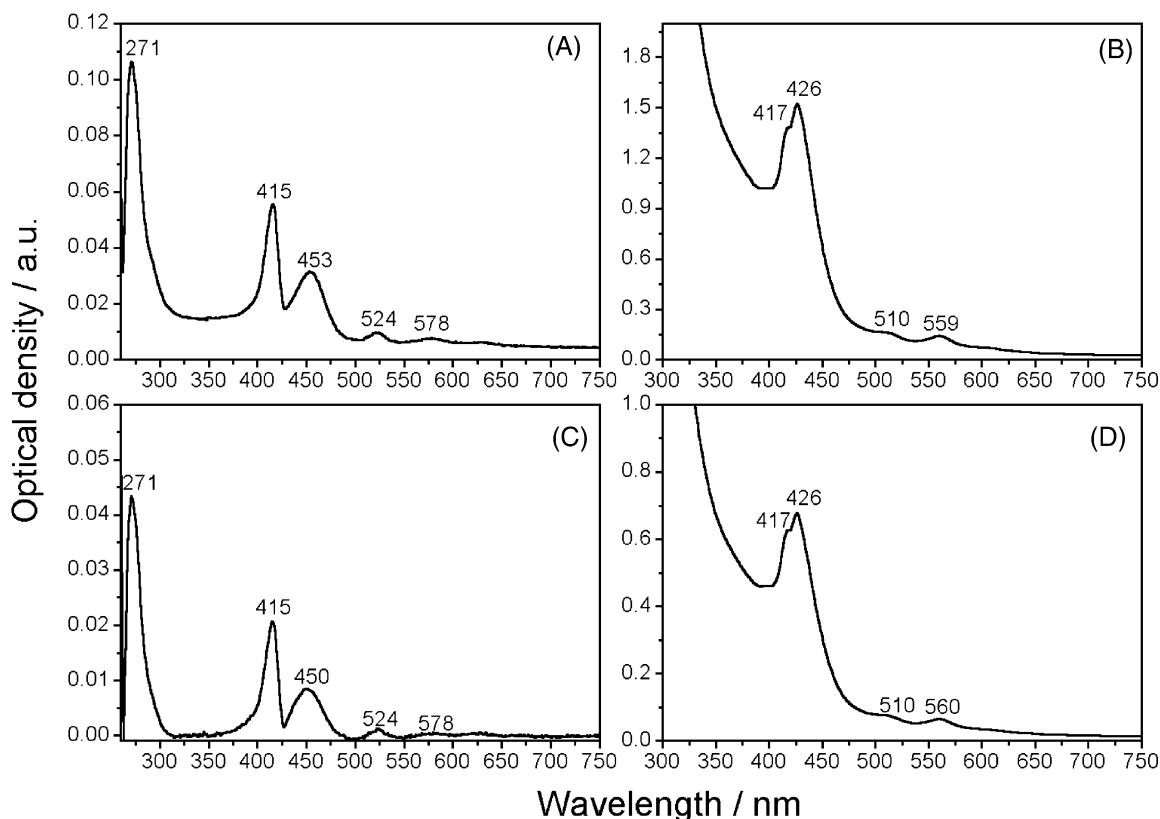


Fig. 3. Absorption of investigated samples in DMF solutions. (A) PPor,  $c = 0.17 \mu\text{M}$ ; (B) PPorV,  $c = 8.4 \mu\text{M}$ ; (C) PPor + EDTA,  $c = 0.07 \mu\text{M}$ ; (D) PPorV + EDTA,  $c = 3.7 \mu\text{M}$ .

of filtration, the amount of the free dye and/or small parts of polymer with only one dye molecule attached, strongly increases. In the latter case, the interaction between  $\pi$  systems of dye molecules decreases.

The absorption obtained for filtered PPor sample (not shown) is very similar to previously reported absorption [16] for a free (not connected with polymer), dye. This suggests that during the sample storage, a small part of the dye molecules is separated from polymer, and/or that short parts of polymer with only one dye molecule attached are formed. After some hours, equilibrium between all forms is reached and the samples become stable, because the absorption and fluorescence spectra no longer change, even during the illumination necessary for the measurements.

Investigations of the filtered solutions were carried out for all samples in order to show the influence of dye attachment to polymer. These results will be described only in brief in the text. Most of the results presented concern the samples with absorption such as in Fig. 3.

Based on a comparison of the absorption spectra of PPor with PPorV we see that the covalently linked viologen changes the shape of absorption spectra. The amount of viologen units linked to polymer is much higher than the amount of porphyrin units. Viologen absorption is located in a short wavelength region ( $\lambda < 200$  nm and in the region of 250–300 nm with the maximum at about  $\lambda = 285$  nm) [31]. The photoreduced viologen absorbs at 600–605 and 380–399 nm regions and a band at about 490 nm is due to reduced viologen dimer [9,32]. In a short wavelength region (250–370 nm), the polymer absorption and two porphyrin maxima of absorption of higher excited electronic states are also located. The porphyrin M band is at about 270 nm, and the L band at 375 nm. The B band is usually in a visible range (at about 416 nm for monomeric pigment) [16,33]. The linking of the large groups to porphyrin or interaction of this dye with phospholipids [21,34] causes the shift of B band to 427 nm. The arrangement in monolayers reaches even 440 nm [34,35]. The strong differences between PPor

(Fig. 3A) and PPorV (Fig. 3B) may be due not only to the absorption of viologen as such, but also to the formation of new forms of porphyrin and viologen as a result of their mutual interactions [9,10]. In these interactions, the polymer can have an important role [17,18]. The positions of the absorption spectra maxima are collected in Table 1. In all samples two maxima in the Soret band are observed. Based on a comparison with “filtered” samples absorptions (not shown), one can see that the maxima at 415–417 nm range are due to forms more weakly interacting with polymer than forms absorbing at longer wavelengths.

The comparison of Fig. 3A with Fig. 3C as well as Fig. 3B with Fig. 3D shows that the addition of EDTA to DMF solutions does not change the shape of the absorption spectra. The TEA addition also has no influence on the absorption spectra. It shows that electron donation from EDTA to ground state of PPor is not observed and electron transfer from porphyrin to viologen is not efficient. The samples with EDTA addition were diluted twice, but this has no influence on the shapes of the absorption spectra. This shows that aggregation effects can be neglected.

In order to check the interaction of electron donors on excited states spectra the absorption of PPorV with addition of EDTA and with TEA under Ar atmosphere before and just after strong illumination was measured (Fig. 4). As it follows from Fig. 4 the illuminated spectra of sample TEA electron donors is followed by the creation of reduced forms of viologen with absorption in 600–750 nm region. Using EDTA it is difficult to record such changes, may be because of low solubility of EDTA in DMF. A different situation is observed when a small amount of free viologen was added to the samples (Fig. 4). In this case, the irradiation, for the samples with both electron donors, causes the creation of new maxima in a range 550–750 nm and as additional peak at 399 nm. According to literature [9,32] these peaks correspond to the reduced viologen monomer, whereas reduced viologen dimer absorption is located at about 490 nm. The peak at 490 nm is not observed. The weak changes in absorption

Table 1  
Absorption and fluorescence maxima in nm of the samples, short wavelength maxima (SWM), concentration in  $\mu\text{M}$  ( $c$ )

Sample	$c$ ( $\mu\text{M}$ )	Absorption					Fluorescence <sup>a</sup>		
		SWM	Soret (B)	$Q_y(0,1)$	$Q_x(0,1)$	$Q_x(0,0)$	SWM	$Q_x(0,0)$	$Q_x(1,0)$
PPor	0.17	236 ~272 293 337	415 ~455	524	~579	627	320	639	–
PPor + EDTA	0.07	271	415 450	524	578	–	316	638	–
PPorV	8.4	236 285 ~300	417 ~428	510	~560	–	530	618 643	709
PPorV + EDTA	3.7	~300	417 426	510	560	–	532	620 643	708

<sup>a</sup> Concentration as given in legends of Figs. 6 and 7.

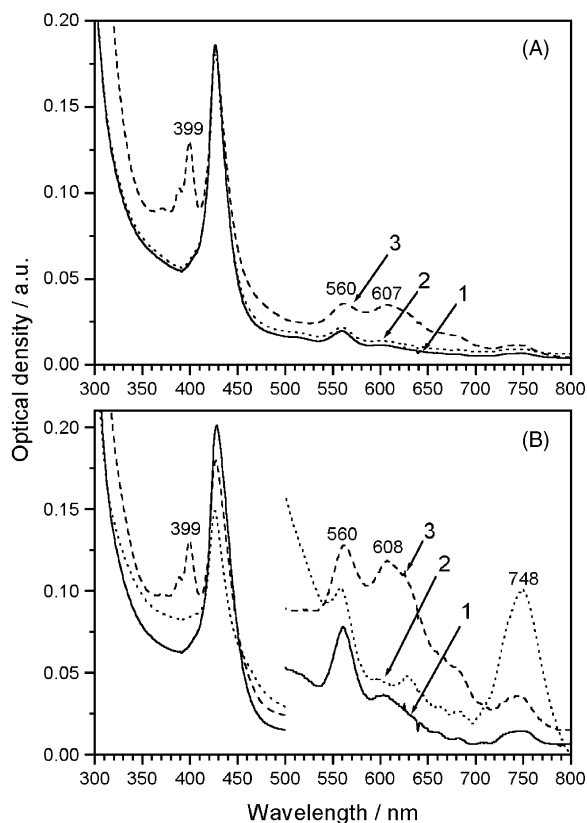


Fig. 4. Absorption of PPorV in DMF with electron donor addition, under Ar atmosphere. Before (curve 1) and after strong illumination (curve 2). Curve 3 with methyl viologen addition to solution. (A) electron donor EDTA, (B) TEA.

spectra of viologen and porphyrin attached to polymer may be due to the low possibility to be close to each other, thus the electron transfer from irradiated porphyrin to viologen is not efficient. Free viologen can interact with porphyrin and therefore the reduced forms can be more easily observed.

### 3.2. Fluorescence spectra

In order to check the possibility of excitation energy transfer from polymer to chromophoric groups, the absorption and fluorescence excitation spectra of polymer alone located in two solvents were measured (Fig. 5A and B).

Fig. 6 shows the fluorescence spectra of PPor (Fig. 6A) and PPor + EDTA (Fig. 6B) and the fluorescence excitation spectra of the same dyes (Fig. 6C and D). The fluorescence maxima at 320 and 316 nm (Fig. 6A and B) could belong to polymer emission. These emission maxima are high at the excitation in a polymer absorption region (at 270 nm). The excitation in a porphyrin-polymer absorption region (at 450 nm) gives emission at 638 nm. The excitations in the lower absorption band range gives maxima, located in the same region, but of course with lower intensity. The excitation in the free dye (Por) absorption range (415 nm) gives predominantly ET to PPor (followed by fluorescence at 638 nm) and eventually very low emission seen as a shoulder emission of free Por (located according to [16] at 649 nm). Some weak long wavelength fluorescence (in 680 nm range) is also observed, but it is not excited by 415 nm (Fig. 6).

The EDTA addition (Fig. 6B and D) has no influence on fluorescence and fluorescence excitation spectra. During the observation of excitation spectrum at 320 nm the maxima at 277–279 nm (Fig. 6C) or 296–288 nm (Fig. 6D), which

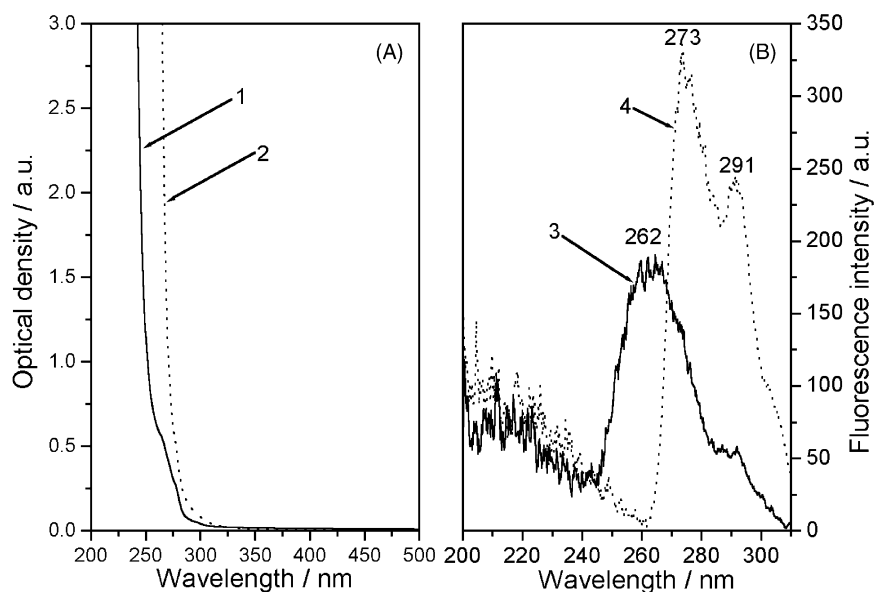


Fig. 5. Absorption (A) and fluorescence excitation spectra (B) of polymer in  $\text{CHCl}_3$  (curves 1 and 3) and in DMF (curves 2 and 4). Fluorescence emission observed at 320 nm.

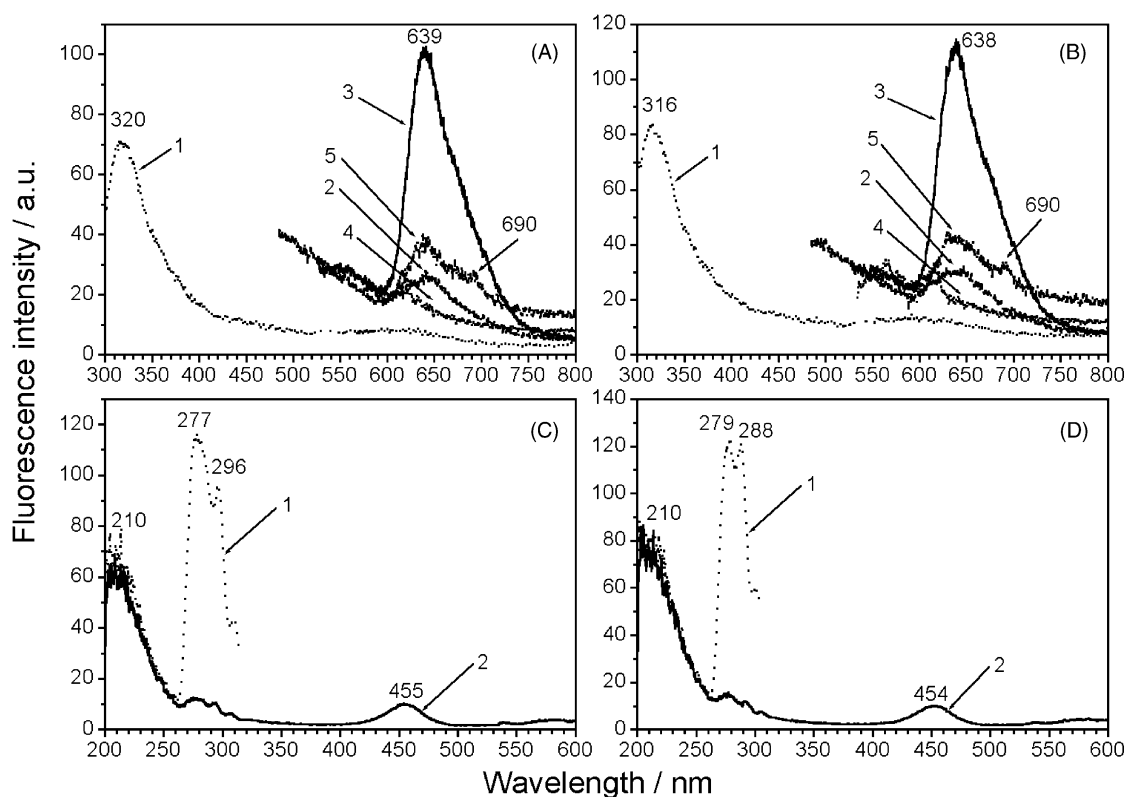


Fig. 6. Fluorescence (A) and (B) and fluorescence excitation (C) and (D) spectra of PPor without EDTA (A) and (C) and with EDTA (B) and (D). Excitation wavelengths in (A) and (B): curve 1, 270 nm; curve 2, 415 nm; curve 3, 451 nm; curve 4, 525 nm; curve 5, 578 nm. Intensities for curves 2–5 are multiplied 10 times. Wavelengths of fluorescence observation: in (C) curve 1 at 320 nm, curve 2 at 639 nm; in (D) curve 1 at 316 nm, curve 2 at 638 nm. Concentrations of samples: in (A) and (C) 0.06  $\mu\text{M}$ ; (B) and (D) 0.04  $\mu\text{M}$ .

are very similar to the maxima observed for absorption of the polymer without dyes in the same solvent (Fig. 5B), are seen. Observation in the porphyrin range of fluorescence gives similar but much lower maxima, in fluorescence excitation spectra Fig. 6C. This shows that in PPor samples, the excitation of polymer is transferred to fluorescent porphyrin chromophores.

The PPorV fluorescence spectra (Fig. 7) are much more complicated than that observed for PPor (Fig. 6). The EDTA addition, similarly as in the case of PPor samples, has no strong influence on the fluorescence (Fig. 7A and B) and on the fluorescence excitation (Fig. 7C and D) spectra of PPorV. The emission maxima at 618 and 643 nm are due to the forms absorbing at 417 and 426 nm, respectively (Fig. 3). However, an additional strong, wide emission fluorescence band is also observed at 530 nm region. This emission is effectively excited at 386 nm absorption (Fig. 7C and D). The monomer of viologen absorbs at 200 and 250–300 nm regions [31], but reduced monomer absorption is at about 380–399 nm [32]. This suggests that 530 nm emission is due to such a form. But one can not exclude other possibilities. The absorption of viologen attached to polymer can be different from that of free viologen because some interactions between viologen and polymer can occur even in ground state, as ob-

served for other systems [9,10]. In our samples many viologen groups are connected to polymer (many times more than porphyrin units). Therefore, the adjacent viologen molecules may strongly mutually interact. As a result of illumination, two closely located viologen groups can form excimer ( $\text{VV}^*$ ) which can go to the ground state by 530 nm fluorescence emission. One can exclude the emission of reduced viologen dimers with absorption at about 490 nm [32] because this spectral region is not effective in 530 nm excitation (Fig. 7).

Viologen is an electron acceptor. Therefore, as a result of PPorV illumination some ionic forms can be created as a result of the electron transfer from porphyrin to viologen. It is very characteristic that in PPorV excitation spectra, the maxima of polymer (277 and 296 nm) are not observed. It seems that polymer strongly interacts with viologen and as a result, polymer fluorescence is quenched and the polymer excitation energy is not transferred to porphyrin. Excitation in the short wavelength region (SWR) (270–300 nm) is for PPorV practically not effective in the excitation of fluorescence of porphyrin. Irradiation in SWR, which is rather effective in the case of PPor, is for PPorV much less effective for exciting emission in the 600 nm region, but it gives some emission at the 530 nm region. This supports our supposition that 530 nm emission is related to viologen. The last emission is

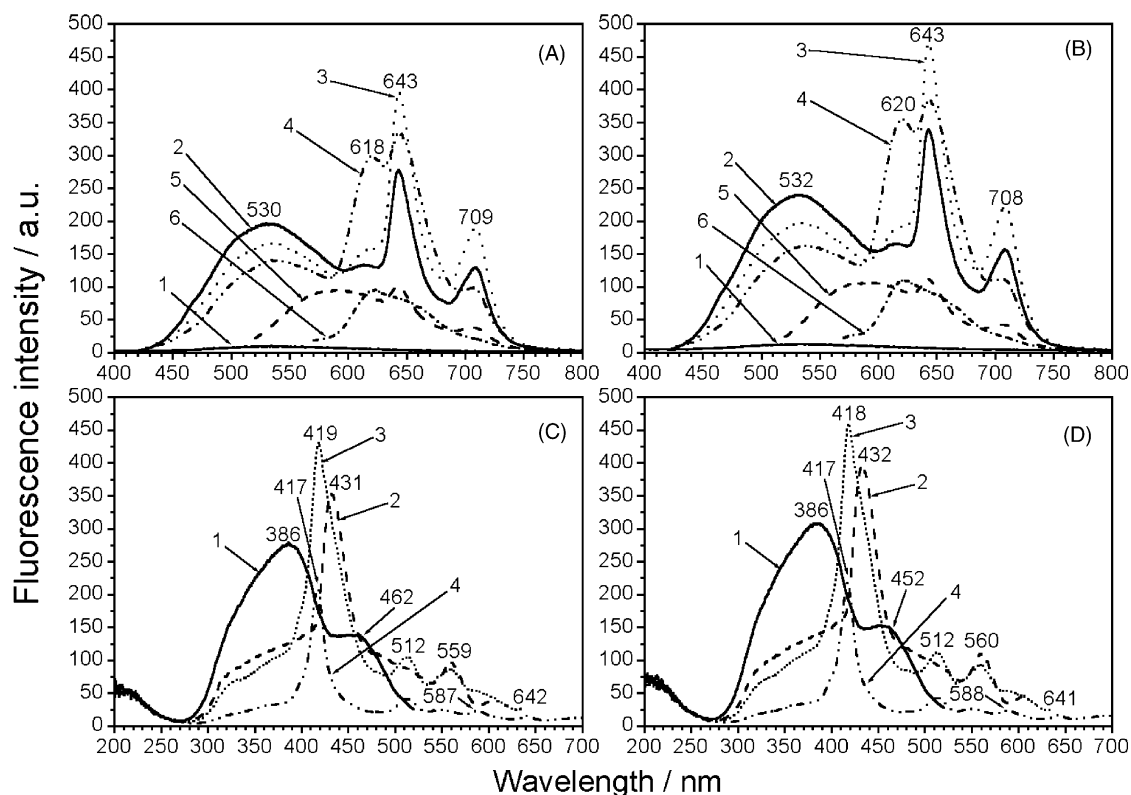


Fig. 7. Fluorescence (A) and (B) and fluorescence excitation (C) and (D) of PPorV without EDTA (A) and (C) and with EDTA (B) and (D). Excitation wavelengths: in (A) and (B) curve 1, 280 nm; 2, 410 nm; 3, 417 nm; 4, 426 nm; 5, 510 nm; 6, 559 nm. In (C) and (D) wavelengths of observation: curve 1 at 530 nm, curve 2 at 619 nm, curve 3 at 644 nm, curve 4 at 709 nm. Concentrations of samples are  $3.2 \mu\text{M}$ .

excited most effectively at 386 nm. In excitation spectra, the maxima of polymer alone (such as in Figs. 5 and 6C and D) are not seen. A form of chromophores absorbing at 386 nm and emitting at 530 nm region are present. The light energy absorbed by polymer and by viologen is transferred to this form emitting the fluorescence in the 530 nm range. Therefore, polymer excitation less effectively reach the porphyrin chromophores emitting at 618 and 643 nm regions.

It is not excluded that the 530 nm fluorescence band can also be to some extent excited by B band of porphyrin (about 410 nm) but it is certain that for the creation of the 530 nm band, the viologen attachment to polymer is necessary. This band is very low in the case of filtered PPorV sample (not shown), which supports the supposition that it is related to covalently linked viologen.

The excitation at 417 nm gives predominantly 643 nm fluorescence, whereas excitation at 426 nm gives emission at the 618–620 nm range. This shows that in PPorV, both porphyrin groups, both weakly and strongly interacting with polymer, are fluorescent.

From the fluorescence and fluorescence excitation spectra of PPorV samples (Fig. 7 and Table 1) it follows that for such samples there is not only very efficient excitation at 418 nm and also at other bands of free porphyrin absorption, but also excitation at about 430 nm (characteristic for porphyrin linked to polymer) is efficient. The ratio of these maxima in

the excitation spectrum depends on the wavelength of fluorescence observation. This shows that porphyrine molecules are present in our samples at least in two different situations, one part strongly interacting between themselves and/or with polymer, the second part is almost free, similar to filtered samples.

### 3.3. Steady state PAS

As it follows from comparison of Fig. 3 (absorption spectra) with steady state photoacoustic spectra (Fig. 8) measured for the same set of samples, the absorption in the 430–450 nm region is followed by especially efficient thermal deactivation. The absorption in this region is observed only in the case of dye connected to long polymer. It is absent in solutions of free dye (“filtered” samples and [16]). This shows that dye chromophores which are strongly interacting with polymer lose much more excitation by exchange into heat than those which are weakly interacting.

The comparison of Fig. 8 with Fig. 3 shows that for most of the samples, the main maximum of PAS is slightly shifted with respect to the absorption maximum. The shapes of main PAS and absorption bands are slightly different. This shows that in the samples the chromophores are located in various environments and therefore they exchange their excitation into heat with different yields. The change in frequency of



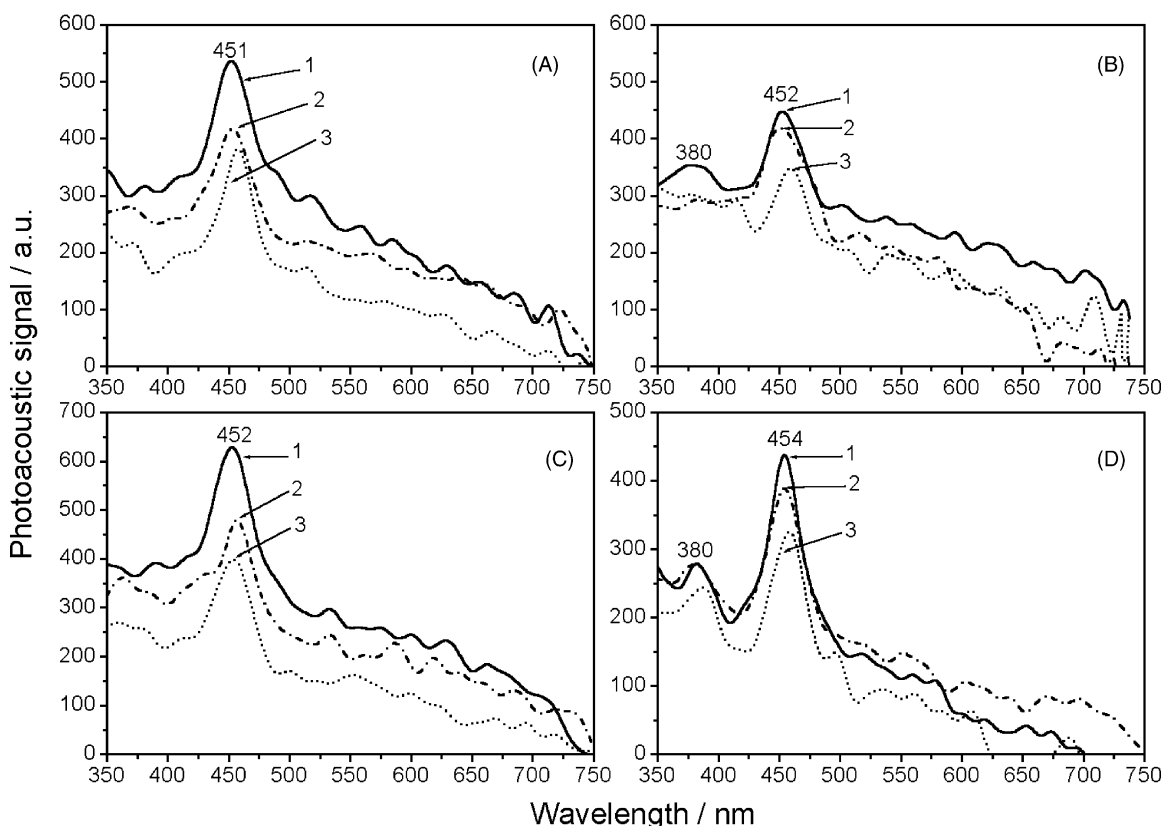


Fig. 8. Steady state photoacoustic (PAS) spectra of (A) PPor, (B) PPorV, (C) PPor + EDTA, (D) PPorV + EDTA. Frequency of light modulation: curve 1, 10 Hz; curve 2, 20 Hz; curve 3, 30 Hz.

light modulation causes only a slow shift of the main PAS band, which suggests that the admixture of a component with slower decay of thermal deactivation is not very large [36]. The relative yields of TD, calculated with respect to the value for PPor, from main maximum of PAS and the absorption in the same region are collected in Table 2. The TD is highest for PPor + EDTA, which exhibits the highest yield of fluorescence (Table 3). It is not observed a regular correlation between yields of TD and fluorescence. There is reasonable because the fluorescence intensity depends not only on absorption of fluorescent dye at excitation wavelength, but also on the absorption of other compounds (polymer, viologen) which can transfer their excitation to fluorescent porphyrin with various efficiency and can exchange their excitation into heat with different yields. At the same

wavelength of excitation the contributions to both processes from various compounds are different for various samples. The observation of PAS maximum in a region 370–390 nm, occurring only in the case of samples with viologen, is very interesting. In this region, absorption of reduced monomeric viologen is located [32]. It appears that such a form is exchanging a large part of absorbed energy into heat because it is better seen in PAS than in absorption spectra.

### 3.4. Laser induced optoacoustic spectra (LIOAS) results

#### 3.4.1. The influence of the volume change of macromolecules on LIOAS

Fig. 9A shows the LIOAS signals for PPorV sample and reference measured at various temperatures, Fig. 9B at various EDTA concentrations and at different times after sample preparation. Higher EDTA concentration causes an increase in  $H_{\max}$ , which shows that the electron donor added to the solution causes an increase in the fast TD processes. Some changes in  $H_{\max}$  are observed in time of sample storage. Therefore, all spectra were measured at a similar time after sample preparation. The absorption spectra of the samples and references change as a function of temperature (for example, in Fig. 10). Therefore, the concentrations at which the absorption of the sample and the reference at the wavelength of laser light (430 nm) are equal, have to be

Table 2

The ratios of the thermal deactivation of various samples with respect to  $TD_R$  of PPor sample, frequency of light modulation ( $\nu$ )

Sample	$TD_S/TD_R$ ( $\nu = 10$ Hz)	$TD_S/TD_R$ ( $\nu = 20$ Hz)	$TD_S/TD_R$ ( $\nu = 30$ Hz)	$TD_S/TD_R$ (average)
PPor	1	1	1	1
PPor + EDTA	3.78	3.71	3.37	3.62
PPorV	2.42	2.91	2.64	2.66
PPorV + EDTA	1.31	1.49	1.36	1.39

Measured at 450 nm.

Table 3  
Values of fluorescence yield  $\phi_F$ ,  $\alpha$  (formula 1) and values of slow TD yield ( $\phi_T$ )

Sample	1			2			3		
	$\phi_F$	$\alpha$	$\phi_T$	$\phi_F$	$\alpha$	$\phi_T$	$\phi_F$	$\alpha$	$\phi_T$
PPor	0.062	0.32	1.23	0.062	0.32	1.23	0.062	0.34	1.09
PPor + EDTA	0.079	0.42	0.93	0.079	0.41	0.95	0.079	0.43	0.91
PPorV	0.013	0.53	0.82	0.013	0.53	0.82	0.013	0.58	0.73
PPorV + EDTA	0.016	0.65	0.60	0.016	0.64	0.62	0.016	0.67	0.56
PPorV + TEA	0.027	0.46	0.92	0.027	0.30	1.21	0.027	0.51	0.83

Accuracy:  $\Delta\phi_F = 0.001$ ;  $\Delta\alpha = 0.04$ ;  $\Delta\phi_T = 0.20$ . (1) In contact with atmosphere; (2) bubbled by nitrogen; (3) bubbled by oxygen.

established at the temperature used for LIOAS measurements. The measurements must be done at such a temperature at which the contributions from the volume changes of the illuminated sample to the measured LIOAS signal can be neglected [28]. As shown in Fig. 9A the ratio of the first large maximum ( $H_{\max}$ ) of the sample and the reference, as well as the shapes of the next smaller maxima change strongly between 30 and 15 °C, whereas they undergo much less significant changes between 15 and 5 °C temperature of sample. Therefore, we suppose that at 5 °C, LIOAS signal is predominantly related to thermal effects and that at such a temperature the volume effect can be neglected. The difference in LIOAS results obtained for the highest (30 °C) and the lowest (5 °C) temperatures was about 20%.

Since we are interested predominantly in the efficiency of triplet states generation the results for 5 °C are the most important to us.

### 3.4.2. Analysis of LIOAS results

From the first maximum of LIOAS measured at 5 °C ( $H_{\max}$  in Fig. 11) using the method elaborated by Marti et al. [26] the part of light energy exchanged into heat in a time shorter than the time resolution of apparatus (0.5  $\mu$ s) and the yield of triplet state generation  $\Phi_T$  are calculated.

$H_{\max}$  was obtained from the following formula:

$$H_{\max} = k\alpha E_{\text{las}}(1 - 10^{-A}) \quad (1)$$

where  $\alpha$  is the part of energy promptly deactivated into heat,  $E_{\text{las}}$  the energy of laser light,  $A$  the absorption of laser light at the wavelength of the laser light (430 nm),  $k$  the coefficient related to the apparatus optical geometry, electronic impedance and thermoelastic properties of the solvent. The  $k$  value is the same for the sample and for the reference,  $\alpha$  for reference is in good approximation equal to 1. The values of  $\alpha$  obtained for the measured samples are gathered in

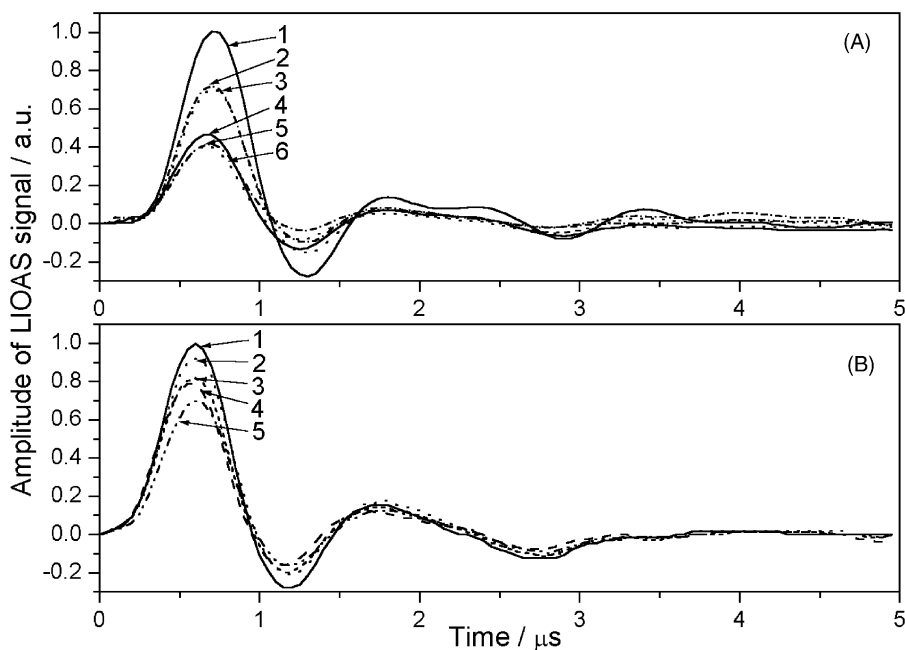


Fig. 9. LIOAS signals (A) of references (curves 1–3) and PPorV (curves 4–6) at various temperatures. Curves 1 and 3 at 30 °C, curves 2 and 5 at 15 °C, curves 3 and 6 at 5 °C. (B) LIOAS signals for PPorV; curve 1, reference; curve 2, PPorV + EDTA in 10 times higher concentration than PPorV; curve 3, PPorV + EDTA at equal concentrations of PPorV and EDTA; curve 4, PPorV just after introduction into DMF; curve 5, the same sample as in curve 4 but 2 days later.

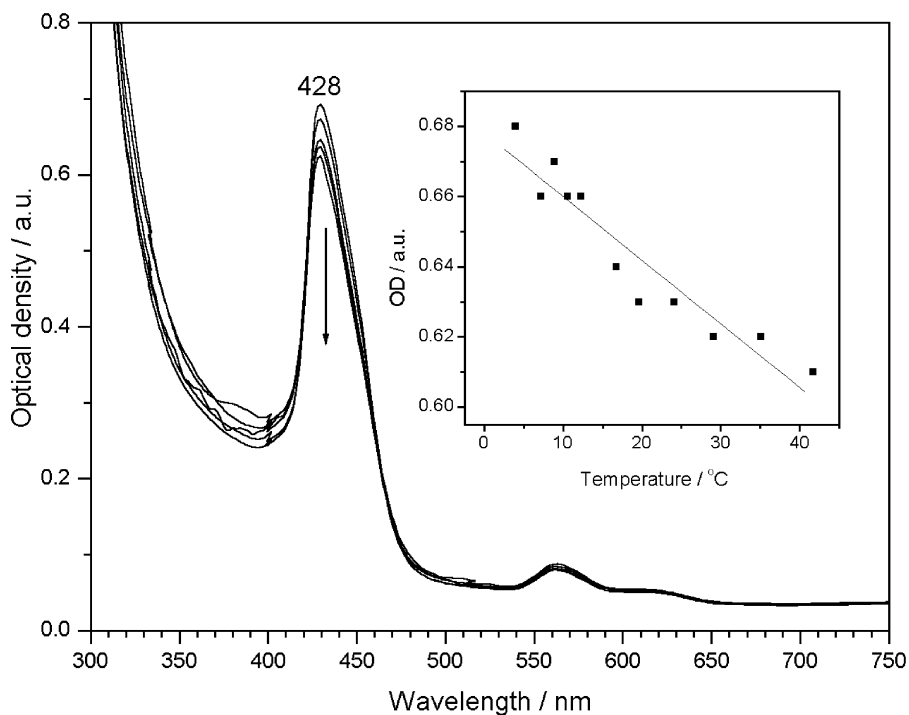


Fig. 10. Absorption spectra of PPorV at various temperatures. Inserts: the dependence of main maxima (at B 428 nm) on temperature.

Table 3 and introduced into the following formula:

$$\Phi_T E_T = (1 - \alpha) E_{\text{las}} - \Phi_F E_F \quad (2)$$

where  $\Phi_T$  and  $E_T$  are the yield of triplet state generation [26] and the energy of triplet state,  $\Phi_F$  and  $E_F$  the yield and energy of fluorescence,  $E_{\text{las}}$  is given in kJ/mol.

The yield of fluorescence was measured according to the method described in [37]. As a reference Rhodamine 6G was used.

From formula (2) the values of the  $\Phi_T$  are calculated (Table 3). Obtained in such a way the yield of slow TD concerns not only the triplet states deactivation but also all

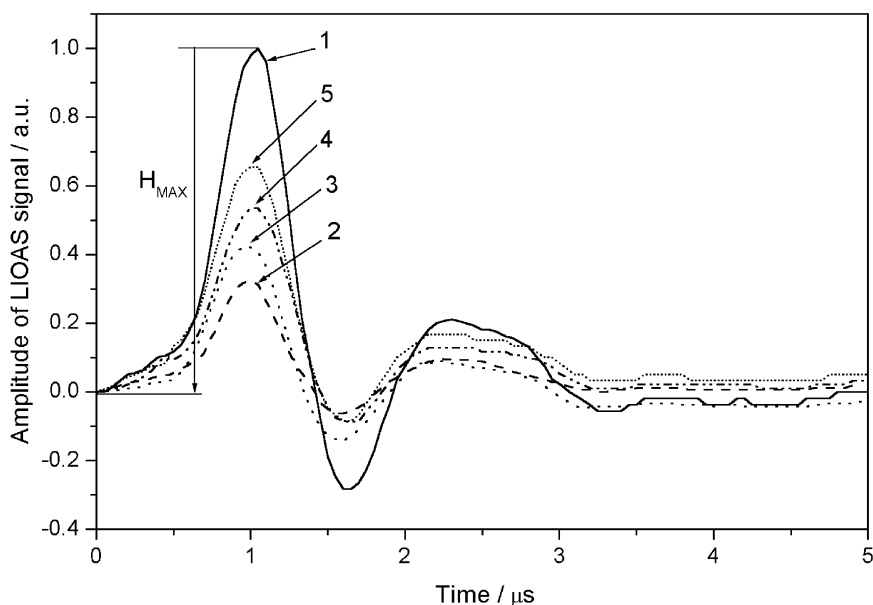


Fig. 11. LIOAS signals of investigated sample measured at 5°C, laser light wavelength 430 nm. Curve 1, reference; curve 2, PPor; curve 3, PPor + EDTA; curve 4, PPorV; curve 5, PPorV + EDTA.

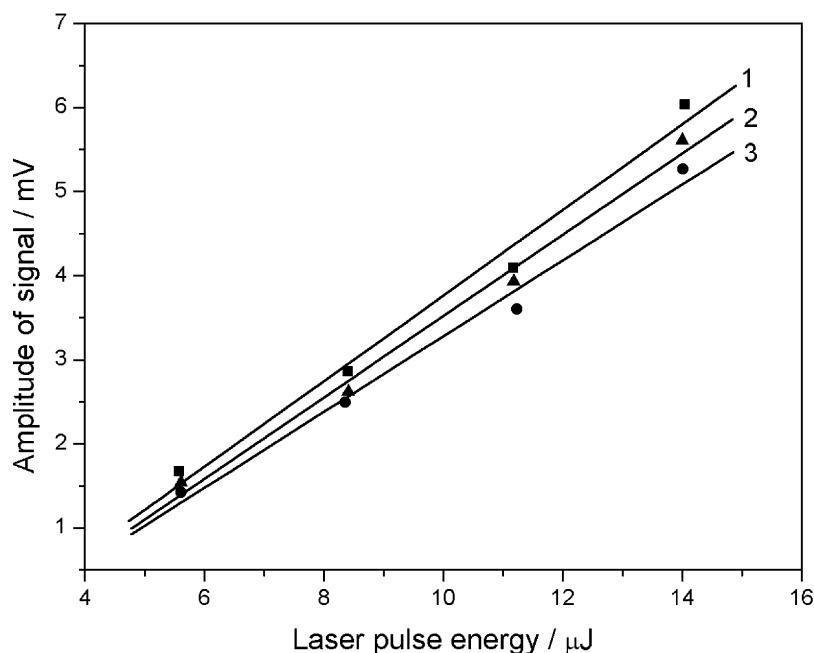


Fig. 12. The dependence of main maximum ( $H_{\max}$ ) of LIOAS signal on the energy of laser flash (at 430 nm) for PPorV solution in DMF for sample bubbled by oxygen (line 1), in contact with atmosphere (line 2) and bubbled by nitrogen (line 3).

exothermic processes delivering heat. Without some information about their decay times it is not possible to establish the source of signals. As one can see from Table 3, the values of  $\alpha$  for samples in contact with atmospheric oxygen and bubbled by oxygen or nitrogen are very similar. The same result follows from Fig. 12, showing for such three types of sample, the dependence of  $H_{\max}$  on the energy of laser flash. The slope of the three lines are similar. EDTA addition causes an increase in prompt TD, which means a decrease in slow processes. For PPorV ( $1 - \alpha$ ), which means contribution to TD from slow processes, is lower than for PPor, and for the filtered samples (not shown) it is lower than for the dyes connected with polymer. This shows that attachment to polymer preserves the quenching of slow processes of TD. The  $\Phi_T$  values in Table 3 are overestimated because the slow TD component contains not only the heat produced by triplet TD but also the heat which can be created in exothermic reactions occurring between various photoproducts, even during a very long time. This problem is solved by LIOAS deconvolution.

The LIOAS signal deconvolution yields the pre-exponential factors of the “prompt” component ( $k_1$ ) and of the slow decaying component ( $k_2$ ), as well as the decay of slow TD component  $\tau_2$  (Table 4). About decay time of prompt component ( $\tau_1$ ) it is known only that it is shorter or equal to time resolution of apparatus. From the decay time of the slow component it follows that it is predominantly due to thermal decay of triplet of chromophores. The triplet states are generated by ISC from the excited singlet states and deactivated predominantly by the nonradiative transition to the singlet ground state. The deactivations by phosphores-

cence and delayed fluorescence are much less probable. As we can see from Table 4, the measurable triplet decay is for PPor samples about 2  $\mu\text{s}$ , and it is a little shorter for PPorV. Bubbling of the sample by nitrogen has no strong influence on  $\tau_2$ , contrary to bubbling by oxygen, which causes its decrease because of the triplet quenching. This decrease is especially strong for PPor without EDTA. The presence of EDTA diminishes the triplet quenching by oxygen for both PPor and PPorV. The TEA addition has stronger influence

Table 4  
Results of the deconvolution of the photothermal signal done according to [21]

Sample	Gas	$k_1$	$\tau_1$ ( $\mu\text{s}$ )	$k_2$	$\tau_2$ ( $\mu\text{s}$ )
PPor	Air	0.30	<0.5	0.03	1.96
	N <sub>2</sub>	0.30	<0.5	0.03	1.96
	O <sub>2</sub>	0.31	<0.5	0.02	0.64
PPor + EDTA	Air	0.39	<0.5	0.11	2.17
	N <sub>2</sub>	0.38	<0.5	0.12	2.16
	O <sub>2</sub>	0.42	<0.5	0.09	2.14
PPorV	Air	0.49	<0.5	0.08	1.55
	N <sub>2</sub>	0.49	<0.5	0.08	1.55
	O <sub>2</sub>	0.52	<0.5	0.05	0.61
PPorV + EDTA	Air	0.58	<0.5	0.13	1.71
	N <sub>2</sub>	0.57	<0.5	0.13	1.72
	O <sub>2</sub>	0.61	<0.5	0.13	1.69
PPorV + TEA	Air	0.47	<0.5	0.11	>5
	N <sub>2</sub>	0.32	<0.5	0.09	>5
	O <sub>2</sub>	0.54	<0.5	0.18	>5

Pre-exponential factor ( $k$ ); decay time ( $\tau$ ).

on  $\tau$  triplet (Tables 3 and 4). The yields of the triplet formation are rather high. Comparing the values of  $(1 - \alpha)$  obtained from Table 3, with the pre-exponential factors  $k_2$  from Table 4, we can see that besides slow TD in a range 0.5–5  $\mu\text{s}$ , characteristic for TD of dye triplets, are some other slower processes of TD. The apparatus is able to measure decay times until about 5  $\mu\text{s}$ . The processes causing the generation of heat with decay in longer times (for example, exothermic photoreactions) are not measurable. From the sum  $(k_1 + k_2)$  we can evaluate such slow reactions: they must be approximately  $(1 - (k_1 + k_2))$ . We can compare such values with  $(1 - \alpha)$  values, obtained on the basis of data in Table 3, giving contributions from all: slow and very slow processes. As we can see from Tables 3 and 4, the largest amount of excitation is lost for very slow reaction for PPor, and the smallest for PPorV + EDTA.

#### 4. Discussion and conclusions

The fate of energy absorbed in investigated systems can be in approximation explained by simplified schemes (Fig. 13). In Fig. 13 higher vibrational bands are not included in absorption and in fluorescence spectra.

The PPor can be excited on several paths and can also be deactivated along several competing paths (Fig. 13A). The polymer (P) can be excited by absorption of 280–290 nm

light and then it can emit fluorescence  $F = 320$  nm or transfer its excitation to PPor unit. This unit can also be excited directly by absorption of 450 nm light, or by ET from “weakly interacting” (Por) form absorbing at 415 nm. The excited to singlet Soret state form (PPor<sup>S\*</sup>) can lose its excitation as heat (TD 450 nm) or by ISC to triplet state (PPor<sup>T\*</sup>). This triplet is deexcited predominantly thermally with decay time  $\tau$  approximately 2  $\mu\text{s}$  (Table 4). Oxygen causes triplet quenching and as a result the decay time is diminished to about 0.6  $\mu\text{s}$ . The addition of a electron donor (EDTA) prevents the oxidation and the decay time becomes longer.

The PPorV can also be excited and deexcited on various paths (Fig. 13B). In this case, the ET from excited reduced viologen attached to polymer (PV<sup>+</sup>) by the absorption at 370–390 nm, deexcited by: (1) 530 nm emission, (2) TD 380 nm or by (3) ET to porphyrins. The character of 530 nm emission is not quite clear. There are several possibilities. For such samples ET from the free polymer (P) to PPorV unit is not observed. The PPorV TD, as it follows from PAS, occurs predominantly from PPor group. The ISC transition of PPorV is followed by triplet state decaying in a slightly faster time than that for PPor and also quenched by oxygen (Table 4). Both types of porphyrins units, i.e. PPorV strongly interacting with polymer and viologen (A = 426 nm, F = 640–710 nm), and weakly interacting Por (A = 417–420 nm, F = 618–620 nm) exhibit their own well-resolved absorption and fluorescence bands.

TEA addition (Tables 3 and 4) has stronger influence than EDTA on TD processes.

From the presented results these conclusions follow:

1. The viologen covalently linked to polymer is creating new forms of the macromolecule, characterized by new maxima in the fluorescence and in the excitation of fluorescence spectra. This is in agreement with literature data [38] reporting that viologen bound to a macromolecular system acts as sensitizer, for example, in the process of the DNA oxidation, creating ionic and radical forms as a result of illumination.
2. The character of 530 nm emission connected with viologen–polymer system is not yet clear, but we hope to explain it in the near future on the basis of spectro-electrochemical investigations [39–41].
3. The attachment of the dye molecules to the polymer changes their spectral and photochemical properties. The spectra of the dye strongly interacting with polymer are different than spectra of almost free dye molecules. The viologen attachment to PPor quenches the polymer emission and blocks the excitation transfer from polymer and from B band of porphyrin to  $Q_x(0,0)$  porphyrin band responsible for fluorescence.
4. The mutual interactions between viologen and porphyrin molecules attached to polymer and free viologen dissolved in solvent with porphyrin attached to polymer are different.

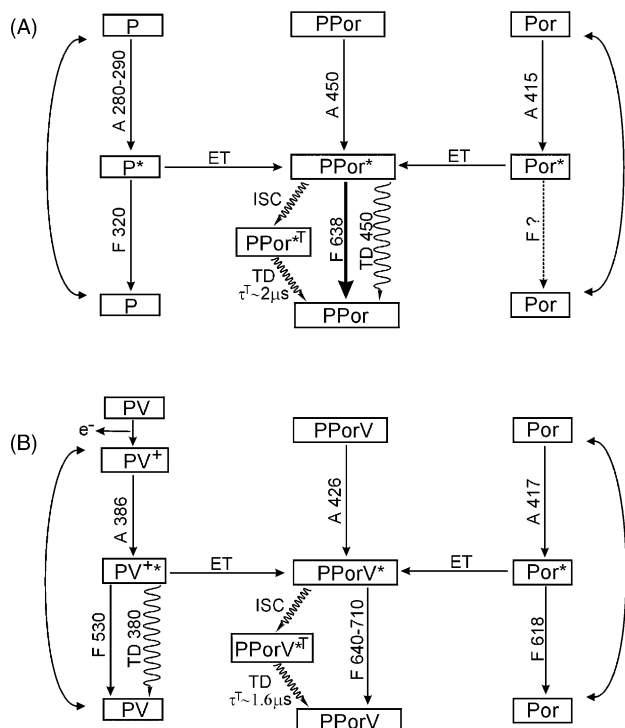


Fig. 13. The scheme of deexcitation of PPor (A); and for PPorV (B); P, polymer; Por, porphyrin group weakly interacting with polymer; PV, polymer with viologen; ISC, intersystem crossing; TD, thermal deactivation; F, fluorescence; A, absorption;  $\tau_T$ , decay time of triplet state.

5. The addition of electron donor (EDTA or TEA) to the solvent (DMF), surrounding the polymer–dye complexes has no measurable influence on singlet states of attached chromophores, but it changes the yield of triplet state generation and triplet thermal deactivation kinetics.
6. Oxygen quenches the triplet state excitations, as it follows from the decrease in the lifetimes of triplet states.
7. The units linked to polymer, similarly as chromophores located in biological macromolecules, change the paths of their deexcitation as a result of changes in their interactions with their surroundings.

## Acknowledgements

Paper was done in a frame of the Japanese, Polish Cooperation Joint Project RJ, 3. Authors (A.B., A.B., J.G., J.L., D.F.) were financially supported by the Poznań University of Technology Grant DS-62-176.

## References

- [1] J.L. Bahr, D. Kuciauskas, P.A. Liddell, A.L. Moore, T. Moore, D. Gust, *Photochem. Photobiol.* 72 (2000) 598.
- [2] D. Frąckowiak, A. Ptak, *Photosynthetica* 30 (1994) 553.
- [3] V.-Y. Lin, S.G. DiMugno, M.J. Therien, *Science* 264 (1994) 1105.
- [4] A. Harriman, J.-P. Sauvage, *Chem. Soc. Rev.* 25 (1996) 1.
- [5] A. Ptak, E. Chrzumnicka, A. Dudkowiak, D. Frąckowiak, *J. Photochem. Photobiol. A: Chem.* 98 (1996) 159.
- [6] D. Frąckowiak, A. Planner, R.M. Ion, K. Wiktorowicz, Near-infrared applications in medicine, in: R. Raghavachari (Ed.), *Near-Infrared Applications in Biotechnology*, Marcel Dekker, New York, 2001, 134 pp.
- [7] N.G. Angeli, M.G. Lagorio, E.A. San Roman, L.E. Dicello, *Photochem. Photobiol.* 72 (2000) 49.
- [8] D. Frąckowiak, J. Goc, A. Waszkowiak, *Curr. Top. Biophys.* 24 (2000) 3.
- [9] Y. Amao, I. Okura, *J. Mol. Catal. A: Chem.* 145 (1999) 51.
- [10] T. Hiraishi, T. Kamachi, I. Okura, *J. Mol. Catal. A: Chem.* 151 (2000) 7.
- [11] D.-J. Qian, S.-O. Wenk, Ch. Nakamura, T. Wakayama, N. Zorin, J. Miyake, *Int. J. Hydrogen Energy* 27 (2002) 1481.
- [12] M. Avron, The electron transport chain in chloroplasts, in: Govindjee (Ed.), *Bioenergetics of Photosynthesis*, Academic Press, New York, 1975, 347 pp.
- [13] A.T. Jagendorf, Mechanisms of phosphorylation, in: Govindjee (Ed.), *Bioenergetics of Photosynthesis*, Academic Press, New York, 1975, 467 pp.
- [14] J. Goc, A. Planner, D. Frąckowiak, L. Vasilieva, M. Hara, J. Miyake, *J. Fluorescence* 9 (1999) 347.
- [15] S.E. Braslavsky, G.E. Heibel, *Chem. Rev.* 92 (1992) 1381.
- [16] D.-J. Qian, A. Planner, J. Miyake, D. Frąckowiak, *J. Photochem. Photobiol. A: Chem.* 144 (2001) 93.
- [17] H.B. Burrows, J. Seixas de Melo, C. Serpa, L.G. Arnoaut, M. da G. Miguel, A.P. Monkman, I. Hamblett, S. Navaratnam, *Chem. Phys.* 285 (2002) 3.
- [18] E. Frankevich, J.M. Muller, U. Lemmer, *Chem. Phys.* 285 (2002) 13.
- [19] A. Kyrychenko, B. Albinsson, *Chem. Phys. Lett.* 366 (2002) 291.
- [20] R.M. Ion, A. Planner, K. Wiktorowicz, D. Frąckowiak, *Acta Biochim. Polon.* 45 (1998) 833.
- [21] D.-J. Qian, Ch. Nakamura, J. Miyake, *Thin Solid Films* 397 (2001) 266.
- [22] P. Hambright, E.B. Flerischer, *Inorg. Chem.* 9 (1970) 1757.
- [23] Y. Okuno, W.E. Ford, M. Calvin, *Synthesis* (1980) 537.
- [24] A. Kelaidopoulou, G. Kokkinidis, E. Coutouli-Argyropoulou, *Electrochim. Acta* 43 (1998) 987.
- [25] D. Frąckowiak, A. Planner, A. Waszkowiak, R.M. Ion, K. Wiktorowicz, *J. Photochem. Photobiol. A: Chem.* 141 (2001) 101.
- [26] C. Marti, S. Nonell, M.T. Nicolaus, *Photochem. Photobiol.* 71 (2000) 11.
- [27] J. Rudzki-Small, L. Libertini, E.W. Small, *Biophys. Chem.* 42 (1992) 29.
- [28] T. Gensch, S.E. Braslavsky, *J. Phys. Chem.* 101 (1997) 101.
- [29] D. Ducharme, A. Tessier, R.M. Leblanc, *Rev. Sci. Instrum.* 50 (1979) 1461.
- [30] D. Frąckowiak, L.G. Erokhina, A. Balter, L. Lorrain, J. Szurkowski, B. Szych, *Biochim. Biophys. Acta* 851 (1986) 173.
- [31] D.-J. Qian, Ch. Nakamura, J. Miyake, *Thin Solid Films* 374 (2000) 125.
- [32] M. Alvaro, H. Garcia, S. Garcia, F. Marquez, J.C. Scaiano, *J. Phys. Chem. B* 101 (1997) 3043.
- [33] V.Z. Paschenko, R.P. Evstigneeva, V.V. Gorokhov, V.N. Luzgina, V.B. Tusov, A.B. Rubin, *J. Photochem. Photobiol. B: Biol.* 54 (2000) 162.
- [34] D.-J. Qian, Ch. Nakamura, J. Miyake, *Langmuir, ACS J. Surf. Coll.* 16 (2000) 9615.
- [35] V.L. Ermolaev, V.A. Lubimtsev, *Acta Phys. Polon. A* 71 (1987) 731.
- [36] M. Pineiro, A.N. Carvalo, M.M. Pereira, A.M.d'A. Roch Gonsalves, L.G. Arnaut, S.J. Formosino, *Chem. Eur. J.* 4 (1998) 2299.
- [37] J. Lakowicz, *Principles of Fluorescence Spectroscopy*, second ed., Kluwer, New York, 1999, p. 52.
- [38] J.R. Rogers, T.P. Le, L.A. Kelly, *Photochem. Photobiol.* 73 (2001) 223.
- [39] W.S. Szubliński, *Inorg. Chem. Acta* 228 (1995) 243.
- [40] J. Goc, D. Frąckowiak, *J. Photochem. Photobiol. A: Chem.* 59 (1991) 233.
- [41] W.S. Baker, B.I. Lemon, R.M. Crooks, *J. Phys. Chem. B* 105 (2001) 8885.